Computerized analysis of coronary artery disease: Performance evaluation of segmentation and tracking of coronary arteries in CT angiograms

Chuan Zhou,[a] Heang-Ping Chan, Aamer Chughtai, Jean Kuriakose, Prachi Agarwal, Ella A. Kazerooni, Lubomir M. Hadjiiski, Smita Patel, and Jun Wei
Department of Radiology, University of Michigan, Ann Arbor, Michigan 48109

(Received 8 September 2013; revised 8 June 2014; accepted for publication 2 July 2014; published 23 July 2014)

Purpose: The authors are developing a computer-aided detection system to assist radiologists in analysis of coronary artery disease in coronary CT angiograms (cCTA). This study evaluated the accuracy of the authors' coronary artery segmentation and tracking method which are the essential steps to define the search space for the detection of atherosclerotic plaques.
Methods: The heart region in cCTA is segmented and the vascular structures are enhanced using the authors' multiscale coronary artery response (MSCAR) method that performed 3D multiscale filtering and analysis of the eigenvalues of Hessian matrices. Starting from seed points at the origins of the left and right coronary arteries, a 3D rolling balloon region growing (RBG) method that adapts to the local vessel size segmented and tracked each of the coronary arteries and identifies the branches along the tracked vessels. The branches are queued and subsequently tracked until the queue is exhausted. With Institutional Review Board approval, 62 cCTA were collected retrospectively from the authors' patient files. Three experienced cardiothoracic radiologists manually tracked and marked center points of the coronary arteries as reference standard following the 17-segment model that includes clinically significant coronary arteries. Two radiologists visually examined the computer-segmented vessels and marked the mistakenly tracked veins and noisy structures as false positives (FPs). For the 62 cases, the radiologists marked a total of 10191 center points on 865 visible coronary artery segments.
Results: The computer-segmented vessels overlapped with 83.6% (8520/10191) of the center points. Relative to the 865 radiologist-marked segments, the sensitivity reached 91.9% (795/865) if a true positive is defined as a computer-segmented vessel that overlapped with at least 10% of the reference center points marked on the segment. When the overlap threshold is increased to 50% and 100%, the sensitivities were 86.2% and 53.4%, respectively. For the 62 test cases, a total of 55 FPs were identified by radiologist in 23 of the cases.
Conclusions: The authors' MSCAR-RBG method achieved high sensitivity for coronary artery segmentation and tracking. Studies are underway to further improve the accuracy for the arterial segments affected by motion artifacts, severe calcified and noncalcified soft plaques, and to reduce the false tracking of the veins and other noisy structures. Methods are also being developed to detect coronary artery disease along the tracked vessels. [http://dx.doi.org/10.1118/1.4890294]

Key words: coronary arteries, vessel segmentation, computer-aided detection, coronary artery diseases, atherosclerotic plaque, multiscale filtering

1. INTRODUCTION

Coronary heart disease (CHD) is a disease in which calcified or noncalcified plaques build up inside the coronary arteries. When the coronary arteries are narrowed or blocked, the reduction of oxygen-rich blood flow to the heart muscle can cause angina or myocardial infarction (MI). Over 16×10^6 Americans have CHD, and over 445000 die of CHD and 151000 die of MI each year.[1] With the rapid advancement of CT techniques, ECG-gated contrast-enhanced coronary computed tomography angiography (cCTA) permits visualization of the vessel lumen, atherosclerotic plaque, and stenoses without the invasive catheterization procedure. cCTA is becoming the most promising modality for assessing CHD and for quantifying the plaques.[2–5] The advent from the 16 row to the latest 320 row multidetector CT not only increases the spatial and the temporal resolution significantly, but also increases the number of images to be interpreted by radiologists substantially. Radiologists have to visually examine each coronary artery for suspicious stenosis using visualization tools such as multiplanar reformation and curved planar reformation provided by the review workstation in clinical practice. These visualization tools depend on the accurate extraction of coronary arteries. Automatic extraction and analysis of the coronary artery trees will reduce the time for interpretation of cCTA.

Accurate identification of plaques is challenging, especially for the noncalcified plaques, due to many factors such as the small size of coronary arteries, reconstruction artifacts caused by irregular heartbeats, beam hardening, and partial volume averaging. Because the plaques only occur in coronary arteries, the extraction of the coronary arteries

constitutes the fundamental step in the detection of plaques. Many of the published studies of vessel segmentation were performed on 2D or 3D images for vascular structures in the retina, liver, brain, and lung. Multiscale filtering has been used for the segmentation of curvilinear or tubular structures in 3D medical images.[6–13] The conventional multiscale filtering method[6,11,14] has been widely used to enhance vascular structures at variable sizes for vessel extraction. In this method, the images are convolved with 3D Gaussian filters at multiple scales and the eigenvalues of the Hessian matrix at each voxel are analyzed in terms of a response function to extract local structures in each scale of the filtered image. The design of the response function is a critical factor that determines the specific shape to be enhanced and therefore whether the multiscale method is effective for a given application. Other methods used in vessel segmentation included hysteresis thresholding,[15] region growing,[16,17] statistical modeling, and matching methods[18,19] using *a priori* knowledge provided by radiologists, direction field based segmentation and detection,[20] and deformable model approaches[21,22] in which an initial surface estimate was deformed iteratively to optimize an energy criterion so that the model boundary was extended to the vessel wall as a so-called minimal surface. Few studies have been conducted for automated segmentation, tracking, and construction of the entire coronary artery trees on cCTA images. In a recent study,[23] a minimum cost path approach was used to extract coronary artery centerline connecting user-defined starting and ending points in cCTA images. Two different cost functions, multiscale vesselness cost function based on eigenvalues of Hessian matrix of images, and region statistics cost function were evaluated. The results show that 88% and 47% of the vessel centerlines were correctly extracted using the vesselness and region statistics cost function, respectively.

We are developing a computer-aided detection (CADe) system to assist radiologists in detecting noncalcified plaques in cCTA scans and automatically identifying the vessels of interest.[24,25] Although commercial visualization workstations have coronary artery extraction software, the digital files of the extracted vessels are not accessible to the users or the researchers. The CADe system has to extract the coronary arterial trees as the first step to define the search space for plaques. In our previous studies,[25,26] we evaluated our prototype multiscale coronary artery response and dynamic balloon tracking (MSCAR-DBT) method for segmentation and tracking of the coronary arterial tree in a small data set and compared the performance of our method with a clinically used commercial workstation that segments and displays coronary arterial trees for radiologist's visualization. The coronary arterial trees in the ECG-gated contrast-enhanced cCTA scans were extracted by our method and the clinical workstation, two experienced cardiothoracic radiologists visually examined the coronary arteries on the original cCTA scan and the corresponding rendered volume of segmented vessels to count the untracked false-negative (FN) segments and false positives (FPs) for both methods. The results indicated that the MSCAR-DBT method was promising with few false negatives and false positives in the small data set. However, the estimated performance might be biased optimistically because it was not evaluated on independent test cases. In this study, we adapted the previously developed 3D MSCAR method for vascular structure enhancement in the heart region, and extensively modified our previous 3D DBT method for the segmentation and tracking of the coronary arteries. The accuracy of our automated method for coronary artery segmentation and tracking was evaluated with an independent test set and quantified by comparison with the coronary arterial trees manually tracked and labeled by experienced cardiothoracic radiologists. False positives were visually judged and marked by the radiologists.

2. MATERIALS AND METHODS

2.A. Data sets

With approval of the Institutional Review Board (IRB), 25 and 62 ECG-gated contrast-enhanced coronary CTA scans were retrospectively collected from patient files in the Department of Radiology for training and independent testing, respectively. All but one cCTA scans were acquired with GE 64-slice (LightSpeed VCT) CT scanners. One test case was acquired with a 16-slice (LightSpeed Pro 16) CT scanner. The image acquisition techniques were 120–140 kVp, 300–600 mAs, and reconstructed at 0.625 mm slice interval. A single reconstructed phase (70% or 75%) was selected for each scan. For the training set of 25 cCTA cases, 21 cases were diagnosed as containing stenosis during the patients' clinical care and 119 plaques were marked by four experienced cardiothoracic radiologists on a computer graphical user interface (GUI) developed in our laboratory. Of the 119 lesions, 12, 50, and 57 were identified as noncalcified soft plaques (NCP), calcified plaques (CP), and mixed calcified and noncalcified soft plaques (MP), respectively. Thirty-six plaques were positive remodeling. Of the 62 cCTA cases in the test set, 50 cases were clinically diagnosed as containing stenosis and 239 plaques were marked by the radiologists, of which 26, 115, and 97 were NCP, CP, and MP, respectively, and 1 with stent installed. Positive remodeling was identified in 87 of the 239 plaques.

For the 62 cCTA cases, three experienced cardiothoracic radiologists provided reference standard for the coronary arteries by manually tracking the arterial trees and marking the center of the arteries using the GUI, as shown in Fig. 1. On the GUI, the sagittal view, axial view, and coronal view of the cCTA scans corresponding to the region where a vessel is being tracked are displayed on the monitor. The GUI has functions allowing the user to scroll through the CT slices, follow the paths of individual vessels, adjust window setting, and zoom to improve visualization. The user can manually track the vessel trees by marking the vessel center points in any one of the three views at each vessel branch and the center point location will automatically propagate to all three views. For each cCTA scan in the test set, 17 major coronary arterial segments[27] that are considered clinically significant can be marked and labeled by name as reference standard for the evaluation of our coronary artery extraction method. The 17 segments include (1) proximal right coronary artery (RCA),

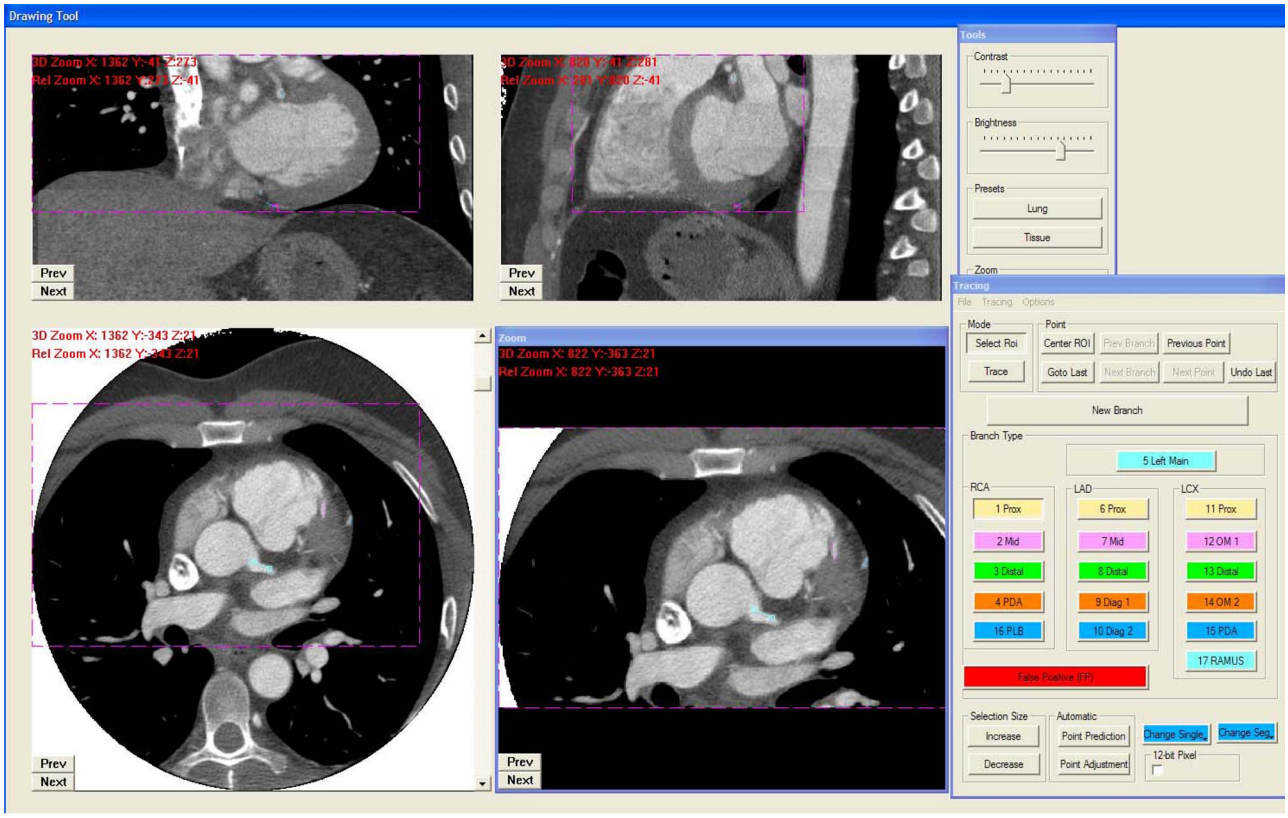

FIG. 1. A screen shot of our in-house developed graphic user interface for manually tracking and marking the center of coronary arteries.

(2) mid-RCA, (3) distal RCA, (4) right posterior descending (RPD) artery, (5) left main, (6) proximal left anterior descending (LAD), (7) mid-LAD, (8) distal LAD, (9) first diagonal, (10) second diagonal, (11) proximal left circumflex (LCX) artery, (12) first obtuse marginal (OM1), (13) distal LCX, (14) second obtuse marginal (OM2), (15) posterior descending (PD), (16) posterior lateral branch (PLB), and (17) ramus intermedius segment, as shown in Fig. 2. For the 62 test cases, total of 10 191 coronary center points were marked on 865 coronary arterial segments by the radiologists, with an average of 13.98 ± 1.12 segments per cCTA scan and 11.8 ± 8.7 points per segment. Some segments could not be tracked because of motion blur or poor contrast filling.

2.B. Methods

Figure 3 shows the schematic diagram of our coronary artery extraction method. In this method, the heart region in the cCTA volume is first extracted. The vascular structures within the heart region are then enhanced using 3D

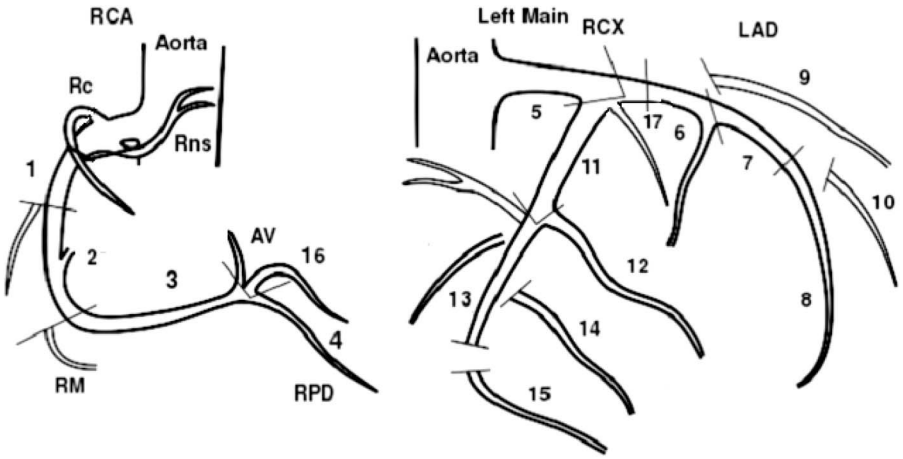

FIG. 2. Seventeen major coronary arterial segments (Ref. 27) that are considered clinically significant. (1) Proximal RCA, (2) mid-RCA, (3) distal RCA, (4) RPD artery, (5) left main, (6) proximal LAD, (7) mid-LAD, (8) distal LAD, (9) first diagonal, (10) second diagonal, (11) proximal LCX artery, (12) OM1, (13) distal LCX, (14) OM2, (15) PD, (16) PLB, and (17) ramus intermedius segment.

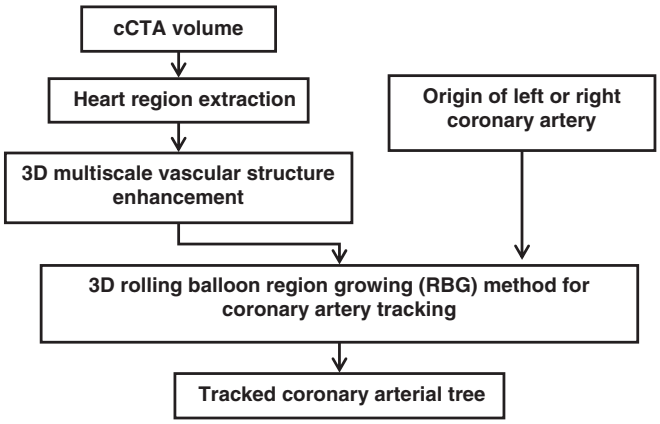

FIG. 3. Schematic diagram of our method for coronary arterial tree segmentation and tracking. All processes are automated except for the initial identification of seed points at the origin of the left and right coronary arteries.

multiscale filtering and the analysis of vessel response function.[26] Starting from the seed points at the origins of the left and right coronary arteries (LCA and RCA), the coronary arteries are segmented and tracked using a 3D rolling balloon region growing (RBG) method. In this study, the entire process was automated after the seed points were manually placed. All methods and parameters were designed with the 25 training cases.

2.B.1. 3D vascular structure enhancement using multiscale coronary artery response method

The heart region is first extracted to reduce computation time and avoid the tracking of the coronary arteries to the pulmonary vessels in the lung region.[26] Gray level thresholding at a voxel value of −970 HU determined by the training set is used to extract the human body from the surrounding air region in the cCTA scan. An adaptive expectation-maximization (EM) segmentation method is then applied to the segmented human body to extract nonair structures including the chest wall, heart, and pulmonary vessels. The heart region is finally extracted by a morphological opening operation applied to the nonair structures with a spherical structuring element. Based on the thoracic anatomy and experimentation with the training set, a 25-mm-diameter spherical structuring element was found to be large enough to shrink the chest wall and pulmonary vessels while preserving the heart in the thoracic cavity because the heart is generally larger than the spherical structuring element of this size.

We have previously developed an MSCAR method[26] for coronary artery enhancement based on the analysis of a vessel enhancement response function specifically designed to extract information from the eigenvalues of Hessian matrices for enhancing coronary vascular structures. In this study the parameters were retrained using 25 training cases. To adaptively enhance the coronary arteries of variable sizes, the response function in the heart region was calculated in K scales by first convolving the heart region with the partial second derivatives of 3D Gaussian functions with a range of variances σ_i^2 ($i = 1, \ldots, K$). To normalize the response function value so that the responses were comparable for the different scales, the output of the convolution with the second derivative of the Gaussian filter at scale i was multiplied by a normalization factor equal to the variance of the Gaussian filter, σ_i^2. The response value at each voxel was determined by the maximum response value over all scales:

$$R_r(x, y, z) = \max\{R_i(x, y, z), i = 1, ..., K\}, \quad (1)$$

where $R_i(x, y, z)$ was the normalized response at scale i and voxel location (x, y, z). In this study, four scales ($K = 4$) were used to cover the coronary arteries over a range from 1.5 to 8 mm in diameter. Figure 4 shows an example of the enhanced vascular structures in a slice of a cCTA volume.

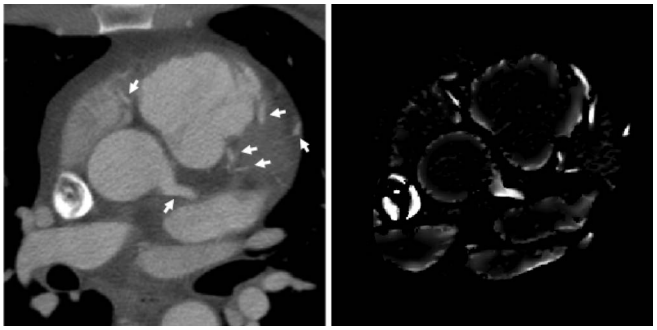

FIG. 4. An example of a slice of cCTA volume with contrast-enhanced coronary arteries (white arrows, left) and structures enhanced using the MSCAR method (right).

2.B.2. 3D rolling balloon region growing method for coronary artery segmentation and tracking

As shown in Fig. 4, the MSCAR method not only enhances the coronary arteries (white arrows) but also enhances the coronary veins, the boundaries of other cardiac structures such as aorta, ventricles, atriums and pulmonary vessels, and other vessel-like noise structures in the heart region. To extract coronary arteries from the enhanced volume of vascular structures, we have developed a 3D RGB method to selectively segment and track the coronary arteries. Given two manually identified seed points located at the origins of the LCA and RCA for each case, the RBG method first refines the seed point location by replacing it with the voxel having the maximum vessel response in a 7-mm-diameter spherical region centered at the initial seed point, then starts tracking the LCA tree or the RCA tree by placing a sphere centered at the refined seed point. Based on the coronary artery anatomy and the observation from our training cases that the sizes of the coronary arteries of adults are smaller than 10 mm in diameter, the diameter of the initial sphere is set to be 15 mm. An adaptive mean-value-based region growing (AMG) method is designed to segment the vessels within the sphere. In the initial sphere, the mean (M_R) of the vascular response value determined by Eq. (1) is calculated in a $5 \times 5 \times 5$-voxel cube centered at the seed point. The vessel inside the sphere is then grown from the seed point based on 26-connectivity and a neighboring voxel P with response value R_p is included in

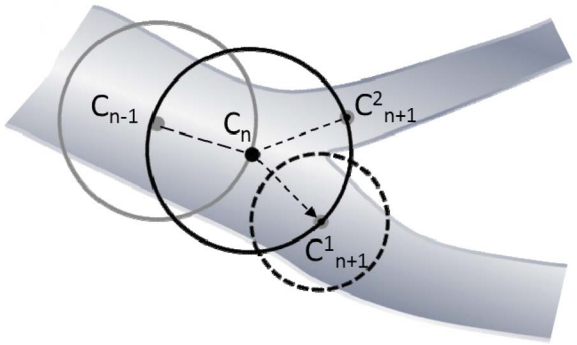

FIG. 5. Illustration of rolling RBG method.

the segmented vessel region if the following growing criterion is satisfied:

$$R_p > (1-t)\,M_R, \tag{2}$$

where t is a tolerance value, empirically chosen using the training set to be 0.2. The mean value is updated as

$$M_R^{v+1} = (vM_R^v + R_P)/(v+1), \tag{3}$$

where v is the number of voxels in the vessel region before the new voxel is added. Figure 5 illustrates our RBG method for vessel growing and tracking. After the vessel region grown in the sphere, the intersections of the sphere surface with the grown vessel are used to determine the size and the location of the next sphere. As shown in Fig. 5, the surface of the current sphere (centered at C_n) rolling from the previous sphere (centered at C_{n-1}) has three intersections with the vessel region grown by the AMG method. The two spheres centered at C_{n+1}^1 and C_{n+1}^2 do not overlap with the already tracked vessel (enclosed by sphere C_{n-1}) so that they are labeled as possible vessels to be tracked next. The next tracking point is chosen from the multiple intersections by finding the center point that has the maximum rolling smoothness:

$$C_{n+1}^{i*} = \arg\max_i(\angle_{n+1}^i * A_{n+1}^i), \quad (i = 1, ..., S), \tag{4}$$

where S is the number of the intersections, $\angle_{n+1}^i$ is the angle between the vector $\overrightarrow{C_nC_{n-1}}$ and the next vector $\overrightarrow{C_nC_{n+1}^i}$, and A_{n+1}^i is the area of the ith intersection. The intersection that has the maximum rolling smoothness with larger angle (between 90° and 180°) and larger intersection area will be chosen as the next tracking point, and the other intersections with the angle between 90° and 180° are labeled as new branches and stored in a queue. The sphere will be rolled and centered at this new tracking point and the diameter of the sphere is adjusted to enclose the local vessel diameter as estimated by the size of the chosen intersection area A_{n+1}^i. As the tracking proceeds along the vessel, a similar vessel growing and search process will be performed at each tracking point, in which the rolling direction is determined by the smoothness of vessel branching and the diameter of the sphere is varied adaptively like a balloon according to the local vessel size. The tracking of each branch continues until there is no intersection with the sphere. The above procedure is then started from a new branch in the queue until the queue is empty.

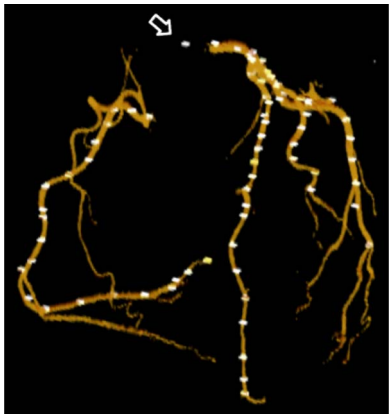

FIG. 6. An example of radiologist-marked center points superimposed on the computer extracted vessels rendered in 3D volume. The center points are enlarged for display purpose.

2.B.3. Comparison studies

Of the 62 test cases, 30 have been used for evaluation of our previous 3D DBT method.[25,26] In this study, we compared the performances between the DBT method and the current 3D RBG method using this subset of 30 cases. In addition, to evaluate the impact of inter-radiologist variability on tracking reference arteries for performance assessment, we performed a comparison study using a subset of 8 cases randomly selected from the 62 test cases. A second experienced cardiothoracic radiologist tracked the coronary arteries based on the 17-segment model independent of the first radiologist's markings. The performances of the RBG method using the two radiologists' tracking separately as reference standards were compared.

3. RESULTS

Figure 6 shows an example of radiologist-marked center points following the 17-segment model that includes clinically significant coronary arteries superimposed on the computer-extracted vessels rendered in 3D volume. For the visible coronary arteries in the 62 test cases, the radiologists marked 10191 center points on 865 coronary segments. The results show that 83.6% (8520/10191) of the manually marked reference points in the coronary arteries overlapped with computer segmented vessels, of which 79.1% (3037/3841) and 86.3% (5483/6350) belong to the RCA tree and LCA tree, respectively. Figure 7 shows the distribution of the reference center points in the 17-segment model and the percentage of the reference center points that overlapped with the computer-segmented vessels for each segment. It can be seen that the major arterial segments including the proximal and distal LAD, the proximal LCX, and the proximal and mid-RCA, can be segmented with higher accuracy (>90% overlap) compared with the segments distal to the above major segments. Using two-tailed unpaired Wilcoxon signed rank test, we found that the differences in the percentages of overlap points were significant ($p < 0.05$) between each of these major segments and the individual distal

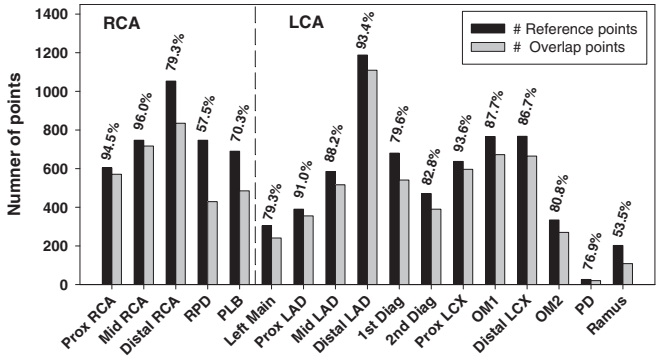

FIG. 7. Distribution of reference points on the 17-segment coronary arteries and the percentages of the reference center points overlapping with the computer-segmented vessels.

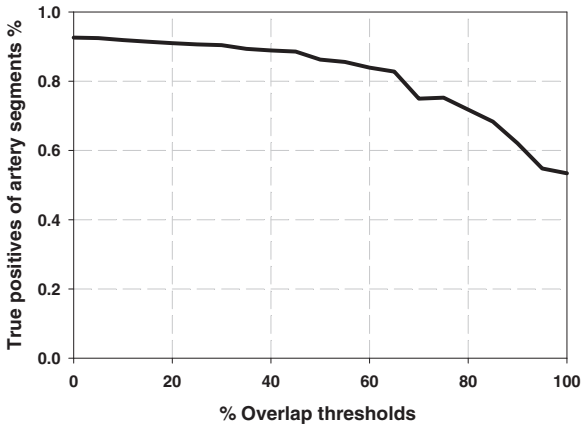

FIG. 8. The fraction of the radiologist-marked coronary segments that were considered to be tracked by the computer (TP) as the POP threshold varied.

segments. The mid-LAD segment had an overlap of 88.2%. As shown in the 17-segment model (Fig. 2), the mid-LAD and distal LAD segments are one continuous branch. Since there was no clear landmark for radiologists to separate the two segments when they manually marked the reference points, one segment could be marked longer and another could be shorter, and vice versa. If the mid-LAD and distal LAD were combined into one segment, 91.7% of the reference points on the combined segment could overlap with computer-segmented vessels.

For each coronary segment, the percentage of the length of the coronary artery segment tracked by the computer is approximated as the percent overlap points (POP), defined as the number of reference center points overlapping with the computer-tracked vessel relative to the total number of reference center points marked by radiologist along that segment, defined as

$$\mathrm{POP} = \frac{\text{Number of reference points on computer} - \text{tracked segment}}{\text{Total number of reference center points along the reference segment}}.$$

As shown in the example of Fig. 6, the computer segmented and tracked vessels could extend beyond the reference segments marked by radiologists. We set the maximum of POP to be 1 such that POP = 1 indicates that the computer segmented vessels are tracked equal to or beyond the reference segment; otherwise, if POP < 1, the specific artery segments are not fully tracked. We define a true positive (TP) segment as a computer-tracked vessel that has a POP greater than a chosen threshold. Of the 865 radiologist-marked segments, 91.9% (795/865) were counted as TPs when the POP threshold was set to be 10%. If the POP threshold was increased to 50% and 100%, the sensitivities were 86.2% and 53.4%, respectively. The 53.4% of TPs at 100% POP threshold indicated that 53.4% (462/865) of computer segmented coronary arteries were tracked equal to or beyond the reference segments marked by radiologists. Figure 8 shows the percentage of the radiologist-marked coronary segments that were counted as TPs when the POP threshold varied. Table I shows, for each of the segments in the 17-segment model, the total number of segments manually marked by radiologists in the 62 test scans, and the average and standard deviation of POP tracked by the MSCAR-RBG method.

Because it is difficult to count false positives (FPs) automatically, for each case, the radiologist visually examined the original cCTA scan and compared the volume rendered computer-segmented coronary arteries to identify mistakenly tracked structures. For the 62 test cases, a total of 55 FPs were identified in 23 cases, including 32 FPs in veins, 10 in the aorta, 2 and 4 in the left and right ventricle, respectively, and 5 and 2 in the left atrial cavity and appendage, respectively. There was no FP identified in 39 test cases. Figure 9 shows examples of different types of FPs from the vessel segmentation and tracking. The segmented arteries that extended beyond the radiologist-marked center points, and the segmented arteries that were not on the list of the 17-segment model but were judged by the radiologists to be a part of the coronary arterial tree were not counted as FP nor TP in this study.

TABLE I. The number of 17 segments manually marked in the 62 test scans by radiologists and the average (Avg) and standard deviation (Std) of POP for each of the 17 segments.

RCA	Prox RCA	Mid-RCA	Distal RCA	RPD	PLB							
Number of reference	61	62	62	58	54							
Avg.	0.940	0.946	0.826	0.649	0.749							
Std.	0.103	0.199	0.286	0.345	0.363							
LCA	Left Main	Prox LAD	Mid-LAD	Distal LAD	1st Diag	2nd Diag	Prox LCX	OM1	Distal LCX	OM2	PD	Ramus
Number of reference	58	61	62	60	58	40	59	60	53	30	3	24
Avg.	0.789	0.926	0.912	0.918	0.737	0.790	0.956	0.845	0.849	0.828	0.800	0.487
Std.	0.177	0.178	0.198	0.210	0.325	0.314	0.107	0.233	0.293	0.341	0.346	0.428

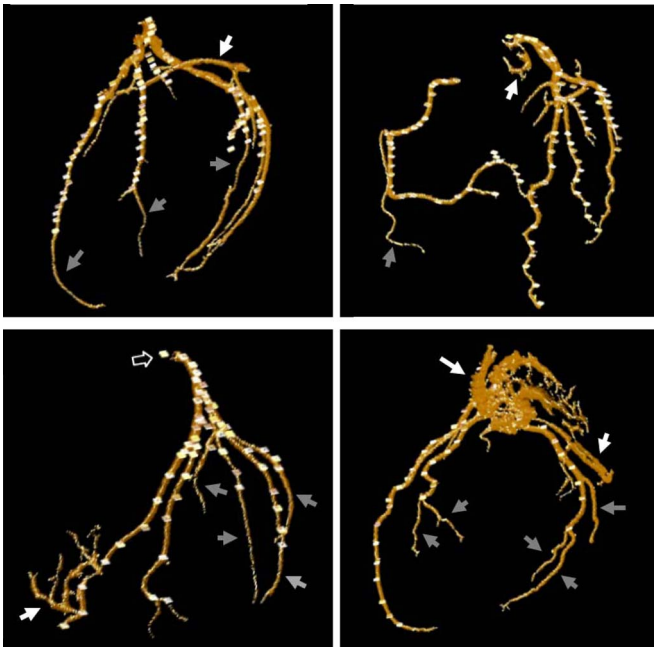

FIG. 9. Examples of FPs extracted by our vessel segmentation and tracking method. The FP structures (white arrows) include vein (top-left), edge of aorta (top-right), right ventricle (bottom-left), left atrial appendage (long arrow, bottom-right), and left atrial cavity (short arrow, bottom-right). The computer-segmented arteries (gray arrows) that extended beyond the radiologist-marked center points or were not on the list of the 17-segment model but were judged by radiologists to be a part of the coronary arterial tree were not counted as FP nor TP.

Figure 10 shows examples of false negative (FN) coronary arteries that were missed by the MSCAR-RBG method. One major reason of FNs was motion blur artifacts. Even with ECG-gating, the reconstructed cCTA images can be degraded by motion blur due to irregular heartbeat of some patients. Motion blur can cause a gap in the vessel being segmented and tracked. If the gap is smaller than the radius of the rolling balloon at that location, there is a chance that the RBG tracking will find the next center point. However, if the gap is long, all segments distal to the blur may be lost, as shown in the examples.

The performances of our previous 3D DBT method[25,26] and the current RBG method for the segmentation and tracking of the coronary arteries were compared using a subset of 30 cases from the 62 test cases. A total of 3487 reference center points on 421 coronary artery segments were marked by radiologists in the 30 cases. The result showed that the DBT-tracked vessels overlapped with 85.6% (2986/3487) of the reference center points. With the RBG method, 89.0%(3104/3487) of the center points overlapped with the tracked vessels. The difference in the number of overlapped reference points per artery segment between the two methods was statistically significant ($p < 0.001$, Wilcoxon signed-rank test). An experienced radiologist identified a total of 28 and 14 FPs in the 30 cases for the previous and current method, respectively. The comparison indicated that both the sensitivity and specificity have been improved with the RBG method.

The impact of inter-radiologist variability on tracking reference arteries for performance assessment was studied in a subset of 8 cases from the 62 test cases. In total, the two radiologists marked 111 segments, and their agreement reached 88.3% (98/111). The 13 segments that were marked by only one of the radiologists were smaller distal arteries including four of the second diagonal, two of the OM1, three of the

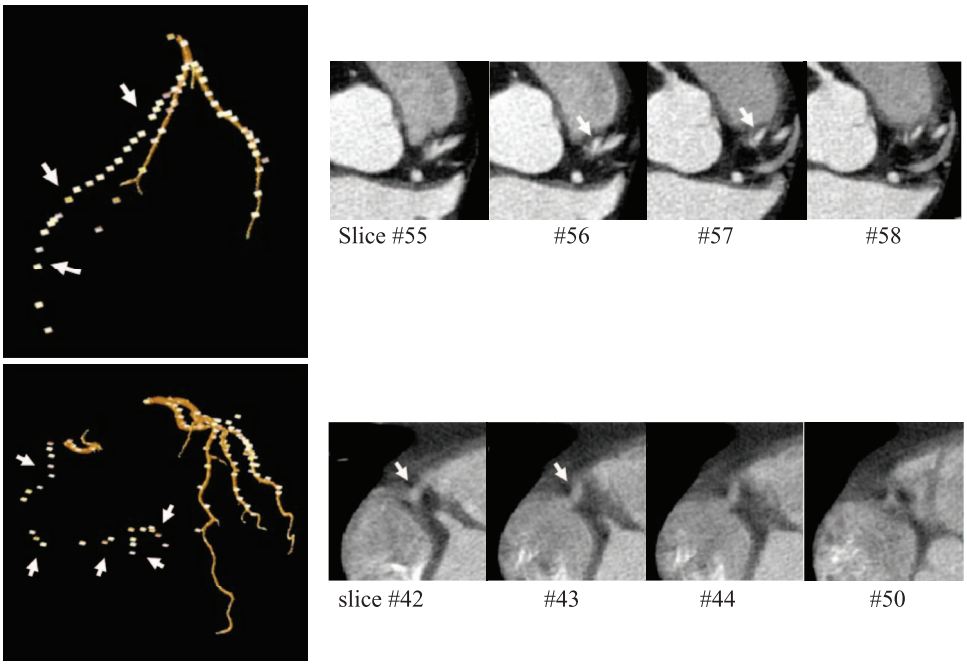

FIG. 10. Examples of failures in the tracking of the LCA and RCA due to motion blur artifacts. Top row: The LAD including proximal, mid, and distal LAD (top left) was not tracked. The motion blur was between slice #56 and 57 (white arrows point to the missed vessel branch in the consecutive axis view). Bottom row: The mid and distal RCA, RPD, PLB, and part of proximal segments were not tracked. The motion blur was in slice #42 and 43.

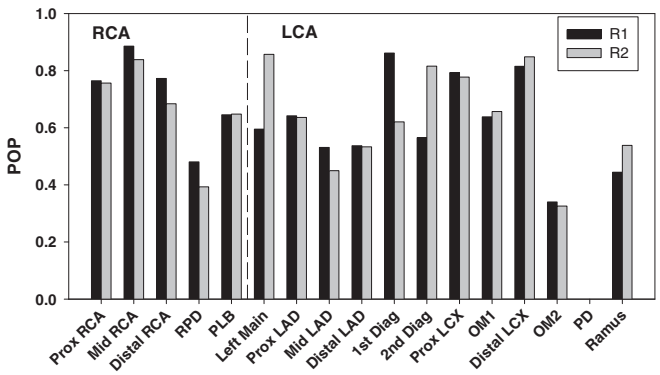

FIG. 11. Comparison between the performance assessments in terms of the POP for the computer-segmented coronary arteries in the 17-segment model using two different experienced cardiothoracic radiologists' (R1 and R2) manually tracked points as reference standard.

OM2, and four of the distal LCX segments. Using the manually marked center points by the two radiologists as reference standard separately, the percent overlap points for the computer-segmented arteries in the 17 segment-model were evaluated and compared, as shown in Fig. 11. The difference of the two methods did not reach statistical significance ($p = 0.891$, two-tailed paired t-test). These results demonstrated that the interradiologist variability may not have a strong impact on the performance assessment in this study, especially for those major nondistal arteries.

4. DISCUSSION

Segmentation and tracking the coronary arteries is a fundamental step to automatically identify the vessels of interest for the development of a computer-aided detection system to assist radiologists in detecting noncalcified plaques in cCTA scans. Many factors, such as vessel blurring caused by irregular heartbeats, narrowing and blockage caused by a significant soft plaque with low-contrast CT value or a calcified plaque with high CT value, incorrect contrast timing, and other noise artifacts can cause the failure of automated vessel tracking. Quantitative evaluation of vessel segmentation accuracy and the completeness of vessel tree construction is challenging because there is no ground truth for the vessel tree in clinical cases. The best alternative to the ground truth of the vessel tree is manual tracing of the vessel center lines by experts. In our previous study[28] that evaluated a pulmonary vessel segmentation method, two experienced thoracic radiologists provided reference standard for the pulmonary vessels including arteries and veins by manually tracking the vessel tree and marking the vessel centers on representative patient cases. However, manual tracking and marking the center points of the vessels are very time consuming. In a pilot study that we compared the relative performance of our prototype system to that of a clinically used commercial software[26] for the segmentation and tracking of coronary arterial trees, quantitative analysis was not feasible because the digital files of the extracted vessel trees by the clinical software were not accessible to the user. As a result, visual assessment was performed to count the untracked FN and mistakenly tracked FP segments for both methods by experienced cardiothoracic radiologists. In this study, we focused on the quantitative evaluation of our current coronary segmentation and tracking method. The reference standard of manually tracked center points of coronary arteries provided by experienced cardiothoracic radiologists allows us to count the TP and FN segments automatically, except that the FPs still needed to be identified and counted manually.

Plaques in an arterial segment will not be detected if the segment is missed in the vessel extraction process. Therefore, whether the coronary artery tree is correctly extracted plays a crucial role in the performance of the CAD system. In our study, the coronary arteries that were not one of the 17 reference segments were ignored and were not counted as FP or FN, as shown in the examples in Fig. 9. For a reference artery segment, the radiologist may not track it to the very distal part beyond certain diameter that was considered clinically insignificant. For the 17 reference segments, the POP measure shows that our method can segment and track the coronary arteries as far as or beyond the reference standard in 462 segments (53.4% of total 865 manually marked segments). Although the plaques not in the 17 segments are not considered clinically significant and may not need to be treated, the detection of plaques in small distal arteries may still be useful for patient management purposes. How far the coronary arteries should be tracked and inspected for plaques would need to be investigated in further studies.

In the framework of Rotterdam Coronary Artery algorithm evaluation,[29] a database of 32 cardiac CTA cases including 8 training and 24 test cases, with corresponding reference standard, is used to evaluate and compare different coronary artery segmentation and tracking methods. In this data set, four major coronary arteries were selected by one observer and manually traced by three trained observers, which are the RCA, LAD, LCX, and a fourth vessel selected from the large side-branches of the above three main arteries. The manually tracked results were merged into reference standards of the centerline and annotated radii along the centerline for each vessel. Four points along the centerline of each selected artery including the starting (S) and ending points (E), and two points (A and B) between the starting and ending points, were provided to the users to identify and guide the segmentation and tracking of the selected arterial branches. Without using these points for the four individual arteries to be tracked, we manually placed two seed points at the origins of the LCA and RCA trees, as required by our algorithm, to track the LCA and RCA trees for each case. The output of our tracking was submitted for evaluation by the Rotterdam framework. Table II shows the evaluation results in terms of three overlap measures (OT, OV, OF) and a distance measure (AI) of our MSCAR-RBG method for the 24 test cases. The exact definitions of the four points and the evaluation measures can be found in the Rotterdam publication[29] and their website. Compared with the reference centerline considered by the Rotterdam framework to be the clinically relevant part of the vessel (the OT measure), our method achieved an average of 91.4% ± 9.0%, which is comparable to the overlap

TABLE II. Summary of Rotterdam Coronary artery algorithm evaluation on the test set for the MSCAR-RBG algorithm.[a]

Case	OV[b] (%)	OT[c] (%)	OF[d] (%)	AI[e] (mm)
8	86.5	89.3	67.2	0.48
9	94.1	95.2	87.7	0.36
10	82.2	83.5	55.1	0.47
11	76.2	76.3	28.7	0.57
12	85.6	89.4	25.2	0.41
13	95.2	96.3	90.9	0.39
14	99.0	99.0	62.0	0.42
15	97.1	98.4	77.1	0.43
16	91.8	96.8	58.2	0.44
17	83.9	85.7	41.7	0.48
18	92.3	93.5	73.9	0.45
19	91.0	95.8	72.6	0.47
20	95.9	96.5	47.2	0.55
21	93.5	97.3	87.9	0.38
22	98.9	99.3	95.5	0.44
23	98.1	98.4	97.2	0.42
24	90.6	93.0	48.2	0.32
25	94.8	96.3	42.3	0.43
26	68.0	69.4	34.5	0.60
27	64.0	64.9	33.1	0.56
28	94.8	96.0	90.1	0.36
29	90.5	93.9	14.7	0.45
30	90.2	93.0	74.2	0.41
31	90.2	95.5	92.5	0.34
Mean ± std dev	89.4% ± 8.9%	91.4% ± 9.0%	62.4% ± 24.6%	0.44 ± 0.07

[a]Evaluation measures defined by the Rotterdam framework.
[b]OV: overlap measure that represents the ability to track the section of the vessel annotated by the human observers.
[c]OT: overlap with the clinically relevant part of the vessel that is defined as vessel segments with a diameter of 1.5 mm or larger.
[d]OF: overlap until the first error that determines how much of a coronary artery has been extracted before making an error. The first error is defined as the first false negative point when traversing from the start of the reference standard to its end while ignoring false negative points in the first 5 mm of the reference standard. A false negative point occurs when a center point found by the algorithm is located at a distance from the reference centerline greater than the annotated radius at that location.
[e]AI: average inside is calculated as the average distance of all the connections between the reference standard and the automatic centerline given that the connections have a length smaller than the annotated radius at the connected reference point.

measure (POP) on our data set for the major vessel segments, i.e., 82.6%–94.0% and 91.8%–92.6%, from the distal to the proximal RCA and LCA, respectively (Table I). For the OV measure, in which the part of the centerline that is correctly tracked by computer but extended beyond the reference endpoint of the manually tracked centerline is counted as FP, our algorithm achieved 89.4% ± 8.9%, indicating that our algorithm could track farther than their manual tracking on average. The OF measure, which determines how much of a coronary artery has been extracted before the first error, is intended to be used for image-guided intravascular interventions and is therefore not relevant to most applications including CAD. In the Rotterdam framework, false positive points along the reference centerlines of these four vessels are scored but other FPs such as the veins, other structures, and artifacts caused by motion and noise elsewhere are not penalized, allowing training to bias toward high sensitivity regardless of specificity due to these FPs. In addition, the Rotterdam framework only evaluates four major arteries, which was selected by one reference observer in that laboratory. These are major limitations of the Rotterdam framework as discussed in their paper.[29] These limitations make the evaluation unfair and impractical for many applications including CAD. Compared with the Rotterdam framework that only evaluates a subset of the major arteries, we evaluated all major coronary arteries in the 17-segment model and FPs using a larger data set of 62 cCTA cases. Our segmentation program was trained taking into consideration the trade-off between sensitivity and specificity as well as the need to extract the smaller, less obvious arterial segments in the 17-segment model. Therefore, comparison of the performance of our method with those of other methods in the Rotterdam framework would require attention to these issues.

In this study, our RBG method used two starting points manually identified at the origins of the left and right coronary arteries as the seed points, respectively, to track the left and right coronary arterial trees for each case. However, the percentage of reference points on the left main artery overlapping with the computer-segmented vessel is smaller than its adjacent segment of proximal LAD (79.3% vs 91.0%), as shown in Fig. 7. This is because, in some cases, the seed points of the RCA were placed at a lower section of the left main and the radiologist started marking the center points at the higher section, as the examples shown in Figs. 6 and 9 (open arrows). We are developing methods for automated detection of the seed point locations at the origins of the LCA and RCA trees. Automated methods for seed point detection may reduce the variability of manually placed seed points.

There are several limitations in this study. First, because the radiologists' manually marked center points were used as reference standard for evaluation of the completeness of the vessel tree segmentation, it is difficult to determine whether the segmented structures that did not overlap with the reference standard points were true coronary arteries, veins, other structures, or simply noise. We therefore were not able to evaluate the FP rate automatically. Each case had to be visually inspected by experienced radiologists to identify and count the FPs, which is time consuming. Without FP assessment, it can be a major bias for intercomparison of different methods such as the Rotterdam framework because methods can usually be trained to achieve higher sensitivity if specificity is not a concern. Further work is needed to design automated methods for characterization and reduction of FPs. Second, manually tracking and marking the center points by radiologists are very tedious and time consuming. We were not able to have multiple radiologists mark each case except for a small subset of eight cases to evaluate interradiologist variations in coronary artery marking and the impact on the performance evaluation of the computerized segmentation and tracking method. However, since the radiologists also visually inspected the tracked vessels to identify FPs, each case was actually read twice by the experienced radiologists. If a major coronary artery segment was missed during marking of the reference center points, the

radiologist inspecting FPs would see the error and make correction. The major variations in the reference standard would likely be how far different radiologists would track each segment, which may affect the POP measure to a certain extent. Third, the seed points for the LCA and the RCA trees were manually placed so that the extraction of the coronary arteries was not fully automated. We have yet to develop an accurate method to automatically identify the origin of the coronary artery trees as seed points. Nevertheless, to our knowledge, this study used one of the largest data sets with radiologists' manually tracked coronary artery trees as reference standards for validation of computerized segmentation and tracking in cCTA.

5. CONCLUSION

Our study demonstrated that the MSCAR-RBG method can accurately segment and track the coronary arteries. Automated and accurate extraction of the coronary arteries is an important step for the development of a computer-aided system for plaque detection and to provide radiologists an efficient visualization tool for vessel analysis in clinical practice. Further studies are underway to develop methods to improve the segmentation and tracking accuracy for the arterial segments affected by motion artifacts, severe calcified and noncalcified soft plaques, and to reduce the false tracking of the veins and other noisy structures.

ACKNOWLEDGMENTS

This work is supported by USPHS Grant Nos. R01 HL106545 and R01 HL092044.

[a]Author to whom correspondence should be addressed. Electronic mail: chuan@umich.edu; Telephone: 734-647-8554; Fax: 734-615-5513.

[1]D. Lloyd-Jones *et al.*, "Heart disease and stroke statistics—2009 update: A report from the American Heart Association Statistics Committee and Stroke Statistics Subcommittee," Circulation **119**, e21–e181 (2009).

[2]J. J. Fine, C. B. Hopkins, N. Ruff, and F. C. Newton, "Comparison of accuracy of 64-slice cardiovascular computed tomography with coronary angiography in patients with suspected coronary artery disease," Am. J. Cardiol. **97**, 173–174 (2006).

[3]M. Budoff *et al.*, "Diagnostic performance of 64-multidetector row coronary computed tomographic angiography for evaluation of coronary artery stenosis in individuals without known coronary artery disease: Results from the prospective multicenter ACCURACY (Assessment by Coronary Computed Tomographic Angiography of Individuals Undergoing Invasive Coronary Angiography) trial," J. Am. Coll. Cardiol. **52**, 1724–1732 (2008).

[4]J. Min, L. Shaw, R. Devereux, P. Okin, J. Weinsaft, D. Russo, N. Lippolis, D. Berman, and T. Callister, "Prognostic value of multidetector coronary computed tomographic angiography for prediction of all-cause mortality," J. Am. Coll. Cardiol. **50**, 1161–1170 (2007).

[5]M. Garcia, J. Lessick, M. Hoffmann, and C. S. Investigators, "Accuracy of 16-row multidetector computed tomography for the assessment of coronary artery stenosis," JAMA **296**, 403–411 (2006).

[6]K. Krissian, G. Malandain, N. Ayache, R. Vaillant, and Y. Trousset, "Model-based detection of tubular structures in 3D images.," Comput. Vis. Image Understand. **80**, 130–171 (2000).

[7]K. Kanazawa, Y. Kawata, N. Niki, H. Satoh, H. Ohmatsu, R. Kakinuma, M. Kaneko, N. Moriyama, and K. Eguchi, "Computer-aided diagnosis for pulmonary nodules based on helical CT images," Comput. Med. Imaging Graph. **22**, 157–167 (1998).

[8]A. F. Frangi, W. Neissen, K. Vincken, and M. Viergever, "Multiscale vessel enhancement filtering," Med. Image Comput. Comput. Assist. Intervent. **1496**, 130–137 (1998).

[9]C. Lorenz, I. Carlsen, T. Buzug, C. Fassnacht, and J. Weese, "A multiscale line filter with automatic scale selection based on the Hessian matrix for medical image segmentation," in *Proceedings of the First International Conference on Scale-Space Theory in Computer Vision* (Springer Berlin Heidelberg, Utrecht, The Netherlands, 1997), pp. 152–163.

[10]S. Aylward and E. Bullitt, "Initialization, noise, singularities, and scale in height ridge traversal for tubular object centerline extraction," IEEE Trans. Med. Imaging **21**, 61–75 (2002).

[11]Q. Li, S. Sone, and K. Doi, "Selective enhancement filters for nodules, vessels, and airway walls in two- and three-dimensional CT scans," Med. Phys. **30**, 2040–2051 (2003).

[12]H. Shikata, E. A. Hoffman, and M. Sonka, "Automated segmentation of pulmonary vascular tree from 3D CT images," Proc. SPIE **5369**, 107–116 (2004).

[13]T. Bülow, C. Lorenz, and S. Renisch, "A general framework for tree segmentation and reconstruction from medical volume data," Med. Image Comput. Comput. Assist. Intervent. **3216**, 533–540 (2004).

[14]Y. Sato, S. Nakajima, N. Shiraga, H. Atsumi, S. Yoshida, T. Koller, G. Gerig, and R. Kikinis, "Three-dimensional multi-scale line filter for segmentation and visualization of curvilinear structures in medical images," Med. Image Anal. **2**, 143–169 (1998).

[15]Y. Masutani, H. Macmahon, and K. Doi, "Automated segmentation and visualization of the pulmonary vascular tree in spiral CT angiography: An anatomy-oriented approach based on tree-dimensional image analysis," J. Comput. Assist. Tomogr. **25**, 587–597 (2001).

[16]G. D. Rubin, D. S. Paik, P. C. Johnston, and S. Napel, "Measurements of the aorta and its branches with helical CT," Radiology **206**, 823–829 (1998).

[17]W. E. Higgins, W. J. T. Spyra, R. A. Warwoski, and E. L. Ritman, "System for analyzing high-resolution three dimensional coronary angiograms," IEEE Trans. Med. Imaging **15**, 377–385 (1996).

[18]R. G. Blanks, M. G. Wallis, and R. M. Given-Wilson, "Observer variability in cancer detection during routine repeat (incident) mammographic screening in a study of two versus one view mammography," J. Med. Screen. **6**, 152–158 (1999).

[19]A. Chung and J. Noble, "Statistical 3D vessel segmentation using a Rician distribution," Int. Conf. Med. Image Comput. Comput. Assist. Intervent. **1679**, 82–89 (1999).

[20]R. Kutka and S. Stier, "Extraction of line properties based on direction fields," IEEE Trans. Med. Imaging **15**, 51–58 (1996).

[21]T. McInerney and D. Terzopoulos, "T-snake: Topology adaptive snakes," Med. Image Anal. **4**, 73–91 (2000).

[22]L. M. Lorigo, O. D. Faugeras, W. E. L. Grimson, R. Keriven, R. Kikinis, A. Nabavi, and A.-F. Westin, "CURVES: Curve evolution for vessel segmentation," Med. Image Anal. **5**, 195–206 (2001).

[23]C. T. Metz, M. Schaap, A. C. Weustink, N. R. Mollet, T. van Walsum, and W. J. Niessen, "Coronary centerline extraction from CT coronary angiography images using a minimum cost path approach," Med. Phys. **36**, 5568–5579 (2009).

[24]C. Zhou, H.-P. Chan, A. Chughtai, S. Patel, L. M. Hadjiiski, B. Sahiner, J. Wei, and E. A. Kazerooni, "Automated segmentation and tracking of coronary arteries in cardiac CT scans: Comparison of performance with a clinically used commercial software," Proc. SPIE **7624**, 76240O (2010).

[25]C. Zhou, H.-P. Chan, J. W. Kuriakose, A. Chughtai, S. Patel, P. Agarwal, E. A. Kazerooni, L. M. Hadjiiski, and J. Wei, "Computerized analysis of coronary artery disease: Performance evaluation of segmentation and tracking of coronary arteries in CT angiograms," in *Proceedings of the 97th Scientific Assembly and Annual Meeting of the Radiological Society of North America*, Chicago, IL, November 27–December 2, 2011.

[26]C. Zhou, H.-P. Chan, A. Chughtai, S. Patel, L. M. Hadjiiski, J. Wei, and E. A. Kazerooni, "Automated coronary artery tree extraction in coronary CT angiography using a multiscale enhancement and dynamic balloon tracking (MSCAR-DBT) method," Comput. Med. Imaging Graph. **36**, 1–10 (2012).

[27]W. G. Austen, J. E. Edwards, R. L. Frye, G. G. Gensini, V. L. Gott, L. S. Griffith, D. C. McGoon, M. L. Murphy, and B. B. Roe, "A reporting system on patients evaluated for coronary artery disease: Report of the Ad Hoc Committee for Grading of Coronary Artery Disease, Council on

Cardiovascular Surgery, American Heart Association," Circulation **51**, 5–40 (1975).

[28]C. Zhou, H. P. Chan, B. Sahiner, L. M. Hadjiiski, A. Chughtai, S. Patel, J. Wei, J. Ge, P. N. Cascade, and E. A. Kazerooni, "Automatic multiscale enhancement and hierarchical segmentation of pulmonary vessels in CT pulmonary angiography (CTPA) images for CAD applications," Med. Phys. **34**, 4567–4577 (2007).

[29]M. Schaap *et al.*, "Standardized evaluation methodology and reference database for evaluating coronary artery centerline extraction algorithms," Med. Image Anal. **13**, 701–714 (2009).